

A Nickel-Cobalt-sensing ArsR-SmtB Family Repressor

CONTRIBUTIONS OF CYTOSOL AND EFFECTOR BINDING SITES TO METAL SELECTIVITY*

Received for publication, July 30, 2002

Published, JBC Papers in Press, August 5, 2002, DOI 10.1074/jbc.M207677200

Jennifer S. Cavet‡, Wenmao Meng‡, Mario A. Pennella§, Rebecca J. Appelhoff‡,
David P. Giedroc§¶, and Nigel J. Robinson‡¶

From the ‡Biosciences, Medical School, University of Newcastle, Newcastle NE2 4HH, United Kingdom and the §Department of Biochemistry and Biophysics, Center for Advanced Biomolecular Research, Texas A & M University, College Station, Texas 77843-2128

NmtR from *Mycobacterium tuberculosis* is a new member of the ArsR-SmtB family of metal sensor transcriptional repressors. NmtR binds to the operator-promoter of a gene encoding a P₁ type ATPase (NmtA), repressing transcription *in vivo* except in medium supplemented with nickel or, to some extent, cobalt. In a cyanobacterial host, *Synechococcus* PCC 7942 strain R2-PIM8(*smt*), NmtR-mediated repression is alleviated by cobalt but not nickel or zinc addition, while the related sensor SmtB responds exclusively to zinc. Quantification of the number of atoms of nickel per cell shows that NmtR nickel sensitivity correlates with cytosolic nickel contents. Differential metal discrimination in a common cytosol by SmtB (zinc) and NmtR (cobalt) is not simply explained by affinities at equilibrium; although NmtR does bind nickel substantially more tightly than SmtB, it has a higher affinity for zinc than for cobalt and binds cobalt more weakly than SmtB. SmtB is known to bind and sense zinc at interhelical four-coordinate, tetrahedral sites across the C-terminal $\alpha 5$ helices, while absorption spectroscopy of Co(II)- and Ni(II)-substituted NmtR reveals five- and six-coordinate metal complexes. Site-directed mutagenesis identifies six potential cobalt/nickel ligands that are obligatory for inducer recognition but not repression by NmtR, four of which (Asp⁹¹, His⁹³, His¹⁰⁴, His¹⁰⁷) align with $\alpha 5$ ligands of SmtB with two additional His provided by a carboxyl-terminal “extension” (designated $\alpha 5C$). Gel retardation assays reveal that zinc does not allosterically regulate NmtR-DNA binding at concentrations where lower affinity cobalt does. These data suggest that two additional ligands form hexacoordinate metal complexes and are crucial for driving allosteric regulation of DNA binding by NmtR, thereby allowing NmtR to preferentially sense metals that favor higher coordination numbers relative to SmtB.

Cells contain regulatory proteins to detect and respond to deficiency or excess of essential metals to maintain sufficient

atoms to satisfy the requirements of metalloproteins while avoiding toxicity (1). The ArsR-SmtB family of transcriptional repressors associate with the promoters of genes encoding proteins involved in the efflux and/or sequestration of excess metal (2). De-repression occurs when the repressors bind metal effectors coincident with the number of atoms exceeding an optimal cell quota. SmtB-mediated repression is alleviated by Zn(II) (3), ZiaR by Zn(II) (4), ArsR by As(III), Sb(III), and Bi(III) (5), CadC by Cd(II), Pb(II) and Bi(III) (6–8), and CzrA by Co(II) and Zn(II) (9, 10). Clearly these sensors discriminate between different metals *in vivo*, but the factors dictating which inorganic elements elicit responses remain to be defined.

There is rich literature describing metal coordination by numerous small molecules *in vitro* and established theories cataloguing the factors likely to influence metal selectivity *in vivo* (11). The ligand environments of metal ions are also known in a vast array of metalloenzymes (12). The binding sites of enzymes are not only influenced by metal selectivity but also by catalytic constraints, different secondary and tertiary structures, and evolutionary histories. Metalloregulatory proteins have some advantages for exploring metal selectivity *in vivo*. First, selectivity will have been a dominant factor in the evolution from a common ancestor of structurally similar sensors that detect different metals. Second, by associating their target promoters with reporter genes it is possible to monitor metal occupancy *in vivo*. In some, if not all, cells there is an absence of free copper (13), and it is likely that this is also true of several other essential metals including zinc (14). Thus, factors that influence the probability of sensors encountering different labile metal ions are likely to influence metal specificity. For example, metallochaperones assist in the delivery of metals, including nickel (15) to some proteins or target compartments (16), promoting advantageous metal-protein partnerships while inhibiting others *en route*. In a two-hybrid assay, a copper metallochaperone from *Synechocystis* PCC 6803 was shown to interact with copper transporting P₁-type ATPases but not with structurally related zinc or cobalt transporters (17), which illustrates how the specificity of metallochaperone-metalloprotein interactions could define which metals are acquired by which proteins *in vivo*.

To identify the regulatory metal binding sites of SmtB we previously generated mutants of Cys and His candidate ligands. One, or both, of a pair of His residues (105/106) was/were required for metal recognition but not repression (18). Difference electron density maps obtained after soaking apo-SmtB crystals with mercuric acetate suggested two symmetry-related pairs of metal binding sites per dimer (19). A pair of metal sites was located close to the $\alpha 3$ helix within the DNA-binding helix-turn-helix motif and a second pair was formed by four ligands, two from each monomer, bridging antiparallel

* This work was supported by the Biotechnology and Biological Sciences Research Council plant and microbial sciences committee Prokaryotic Responses to Environmental Stress initiative (to W. M. and N. J. R.), The Royal Society (to J. S. C.), the National Institutes of Health (to D. P. G.), and the Robert A. Welch Foundation (to D. P. G.). The costs of publication of this article were defrayed in part by the payment of page charges. This article must therefore be hereby marked “advertisement” in accordance with 18 U.S.C. Section 1734 solely to indicate this fact.

¶ To whom correspondence may be addressed. Tel.: 44-191-222-7695; Fax: 44-191-222-7424; E-mail: n.j.robinson@ncl.ac.uk (for N. J. R.) or Tel.: 44-979-845-4231; Fax: 55-979-862-4718; E-mail: giedroc@tam.u.edu (for D. P. G.).

carboxyl-terminal $\alpha 5$ helices. Fractional occupancies were low (<2%), and it was subsequently established that SmtB binds only one zinc per monomer with affinity K_{Zn} in excess of 10^{11} M^{-1} at equilibrium (20). Substitution of cobalt into the zinc sites of SmtB gave spectral features diagnostic of tetrahedral coordination environments with one or two Cys ligands (20). Zinc and cobalt x-ray absorption spectroscopy (21) coupled with ^{15}N - ^1H NMR perturbation spectroscopy (21) implicate Cys¹⁴, His¹⁸, and Cys⁶¹ in a site designated $\alpha 3\text{N}$ (Fig. 1A). However, Cys variant proteins, deficient in $\alpha 3\text{N}$, retain inducer responsiveness *in vivo* (18) and zinc-dependent DNA dissociation *in vitro* (22). In contrast H106Q SmtB was refractory to zinc-induced disassembly of SmtB-DNA complexes *in vitro* (22) consistent with loss of inducer recognition *in vivo* (18). Occupancy of $\alpha 5$ sites (which include His¹⁰⁶, Fig. 1A) regulates DNA binding by SmtB even though $\alpha 3\text{N}$ sites are occupied in dissociated SmtB (Fig. 1B). In contrast, trigonal thiolate sites adjacent to a predicted helix-turn-helix region are required for inducer recognition by ArsR (23), while a tetrathiolate $\alpha 3\text{N}$ site modulates CadC DNA binding *in vitro* (8, 24) and CadC inducer recognition *in vivo* (7). Different allosteric sites ($\alpha 3\text{N}$ or $\alpha 5$) with distinct ligand sets and geometries correlate with, and presumably contribute toward, the biological metal specificities of individual ArsR-SmtB family members. Analogous observations have been made for *Escherichia coli* Fur homologues, Fur and Zur (25).

To identify ArsR-SmtB sensors with new specificities, sequence databases were searched for *smtB*-related genes adjacent to genes predicted to contribute to homeostasis of other metals. Ten genes were identified in the fully sequenced genome of *Mycobacterium tuberculosis* (26), and Rv3744 was selected due to its proximity to a divergently transcribed gene (Fig. 1C) encoding a deduced protein with similarity to CoaT (27). Genes encoding identical proteins are present in *Mycobacterium bovis* (www.sanger.ac.uk) strain BCG (28). An initial aim of this research was to establish whether the product of Rv3744 binds the adjacent operator-promoter to repress transcription, except in the presence of an excess of some metal. Our data support this, and the genes are designated *nmtR* and *nmtA* (Fig. 1C).

In this paper we show that NmtR represses expression from the *nmt* operator-promoter *in vivo* with repression specifically alleviated by elevated nickel or cobalt, the former being the more potent. Comparative analyses of NmtR and the related zinc sensor SmtB, *in vitro* and *in vivo*, lead to some surprising findings. While SmtB detects different metals relative to NmtR in the same cell, revealing intrinsic differences in these sensors, the host cytosol can also influence biological metal selectivity of these metal sensors. We also show that metal sensor selectivity does not simply correlate with metal affinity at equilibrium, but is instead consistent with a model in which distinct coordination geometries of inducing metal complexes of NmtR versus SmtB drive distinct allosteric pathways to effect regulation of DNA binding in each case.

EXPERIMENTAL PROCEDURES

Bacterial Strains and DNA Manipulations—*Mycobacterium smegmatis* mc²155 and *M. bovis* BCG (Pasteur) were used as mycobacterial hosts, and *Synechococcus* PCC 7942 strain R2-PIM8(*smt*) (29), lacking functional *smtA* and *smtB* genes, was used as a cyanobacterial host. The *smtB*-deficient status of the latter alleviates any influence of SmtB (with a similar recognition helix to NmtR) on expression from the *nmtA* operator-promoter in this host. Mycobacterial cells were grown with shaking at 37 °C in LB medium (30) containing 0.05% (v/v) Tween 80, and cyanobacterial cells were grown at 30 °C in Allen's medium using conditions as described (29). *E. coli* strains JM109 (Stratagene) and BL21(*DE3*) were used and grown in LB medium. Cells were transformed to antibiotic resistance as described (29–31). Standard DNA manipulations were performed as described by Sambrook *et al.* (30). All

generated plasmid constructs were checked by sequence analysis.

Construction of *nmt-lacZ* Fusions, Site-directed Mutagenesis, and β -Galactosidase Assays—*M. tuberculosis* H37Rv genomic DNA was used as template for PCR with primers I (5'-GAAGGATCCGGCCAA-CATATCAG-3') and II (5'-GAAGAATTCTGGGGTCTGTAAAGCTCG-3') and the amplification product (497 bp) containing the *nmtA* operator-promoter and *nmtR* (Fig. 1C) ligated to pGEM-T prior to subcloning into the *SalI/Bam*H1 site of pLACPB2 (32) or the *Scal/Bam*H1 site of pJEM15 (31) to create transcriptional fusions with *lacZ*. "QuikChange" (Stratagene) site-directed mutagenesis was subsequently used, according to the manufacturer's protocols, to generate derivatives with codon substitutions within *nmtR*: Gln41 to a UAG stop codon; Asp⁵¹, Asp⁹¹, Asp⁹⁹, and Asp¹¹⁴ to Ala; and His⁹³, His¹⁰⁴, His¹⁰⁷, His¹⁰⁹, and His¹¹⁶ to Arg. The pLACPB2- and pJEM15-based constructs were introduced into cyanobacterial and mycobacterial hosts, respectively. R2-PIM8(*smt*) containing *smtB* and the *smtA* operator-promoter in pLACPB2 (3) was used to examine expression from the *smtA* operator-promoter. β -Galactosidase assays were performed as described previously (33), in triplicate on at least three separate occasions. The media were supplemented with various [metal] (described in individual experiments) for approximately 20 h immediately prior to assays. These assays therefore differed from previous reported assays (3, 29, 33), to examine expression from the *smtA* operator-promoter, which used much shorter (2 h) metal exposure times. Maximum permissible [metal] are: 3/75 μM zinc, 1/200 μM cobalt, 9/500 μM copper, 0.15/500 μM nickel, 0.8/0.5 μM silver, 1.5/2.5 μM cadmium, 100/untested μM lead for cyanobacteria/mycobacteria.

Gel Retardation Assays—For these experiments recombinant NmtR was generated as a fusion to glutathione *S*-transferase by subcloning the *nmtR* coding region, generated by PCR using primers II and III (5'-GAAGGATCCATGGGGCACGGGGTCTGAAAG-3') with *M. tuberculosis* H37Rv DNA as template, into the *Bam*HI/*Eco*RI site of plasmid pGEX-6P2 (Amersham Biosciences). Recombinant fusion protein was expressed in *E. coli* JM109, cleaved using precision protease, purified according to manufacturer's protocols, and dialyzed against 10 mM Tris-HCl (pH 7.5), 1 mM EDTA, followed by 10 mM Tris-HCl (pH 7.5). A single prominent band corresponding to the predicted size of NmtR and five residues of glutathione *S*-transferase (13.238-kDa) was detected by PAGE. Crude cyanobacterial cell extracts were prepared as described (33) and protein concentrations determined using Coomassie Blue R-250 (using bovine serum albumin standards). Gel retardation assays were performed (18) with EDTA omitted from buffers unless otherwise stated. The probe in all cases was 71-bp *Xba*I/*Bam*HI fragment from pGEM-T containing the *nmt* operator-promoter region generated by PCR using primers III and IV (5'-GAATCTAGATGGTTAGGCAGCC-3') with *M. tuberculosis* H37Rv DNA as template. Examination of metal-induced DNA dissociation involved adding increasing [Co(II)] or [Zn(II)] to binding reactions containing recombinant NmtR; to check for reversibility 1 mM EDTA was also added to some reactions after 50 min.

Expression and Purification of NmtR—The *nmtR* coding region was amplified by PCR from *M. tuberculosis* H37Rv DNA, using primers 5'-GAACATATGACAAAACCAGTGTGCAGG-3' and 5'-GAAGAAT-TCTGCCTAAGGTGCATCTC-3', ligated to pGEM-T (Promega) prior to subcloning into the *Nde*I/*Eco*RI sites of pET29a (Novagen). Recombinant protein was expressed in *E. coli* BL21(*DE3*), cell lysates prepared (33), and NmtR purified by binding to heparin-Sepharose (CL-4B column, Amersham Biosciences) equilibrated with 10 mM HEPES (pH 7.8), 50 mM NaCl, 1 mM EDTA, 1 mM dithiothreitol and elution into the same buffer but containing 300 mM NaCl; fractionation of pooled eluate on Sephadex G-75 (246 ml); concentration by re-application to heparin-Sepharose in an anaerobic chamber; and final application and elution from Sephadex G-25 (Amersham Biosciences) in 20 mM MES¹ (pH 6.0), 150 mM NaCl. A single prominent band of the anticipated size (12.827 kDa) was detected by PAGE.

Direct Metal Binding of NmtR and SmtB—Titrations of apo-NmtR (≤ 0.05 mol eq of Zn(II) as determined by atomic absorption spectroscopy; $\epsilon_{280} = 4470 \text{ M}^{-1} \text{ cm}^{-1}$) with Ni(II) and Co(II) were monitored by UV-visible optical absorption spectroscopy (600 μM NmtR) or by steady-state tyrosine fluorescence (for Ni(II), Co(II), and Zn(II); 5.0 μM NmtR) in 10 mM HEPES (pH 7.0), 450 mM NaCl, 22 °C essentially as described previously for SmtB (20, 21). To monitor Zn(II) binding in competition between SmtB and NmtR, Co(II)-SmtB was titrated with Zn(II) in the presence and absence of stoichiometric apo-NmtR and the optical spectra recorded as described and used to monitor bleaching of Co(II)-SmtB complexes. To prepare Co(II)-SmtB, recombinant apo-SmtB was ex-

¹ The abbreviation used is: MES, 4-morpholineethanesulfonic acid.

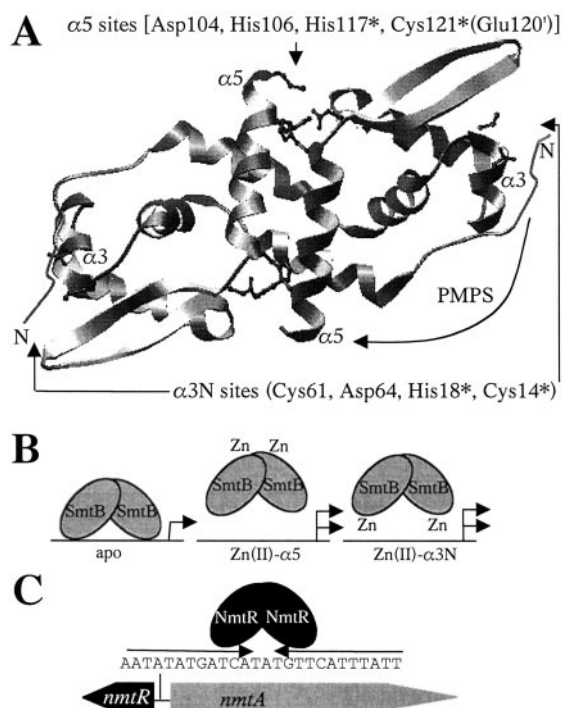


FIG. 1. Metal binding sites of SmtB and physical map of the *nmtR* and *nmtA* genes from *M. tuberculosis*. *A*, residues assigned (21) to $\alpha 3N$, $\alpha 5'$, and $\alpha 5$ sites are indicated on a ribbon representation of the apo-SmtB homodimer (19), with * representing ligands contributed by the second monomer. Glu¹²⁰ or Cys¹²¹ donate the fourth ligand to Co(II) or Zn(II) at $\alpha 5'$ or $\alpha 5$, respectively. *p*-(Hydroxymercuri)phenylsulphonate (PMPS) causes occupancy of $\alpha 5'$. *B*, in the model, apo-SmtB binds the *smt* operator-promoter inhibiting *smtA* transcription, Zn(II) binds at $\alpha 5$ (K_{Zn} $7.8(+1.9) \times 10^{11} \text{ M}^{-1}$) (21) causing DNA dissociation and transcription prior to migration to $\alpha 3N$ ($K_{Zn} \geq 10^{13} \text{ M}^{-1}$) (22). *C*, the *nmtR* and *nmtA* genes from *M. tuberculosis*, corresponding to open reading frames Rv3744 and *ctpJ*, respectively, in the *M. tuberculosis* genome (26), are shown. NmtR is predicted to bind to nucleotides within a degenerate 12-2-12 inverted repeat (sequence shown in full) within the *nmt* operator-promoter region that separates *nmtR* and *nmtA*.

pressed from pET29a, prepared as described for NmtR, and preincubated in an anaerobic chamber with a 4-fold molar excess of Co(II). Studies of competitive metal binding to NmtR (Zn(II) versus Ni(II) versus Co(II)) involved titrating apo-NmtR in 20 mM MES (pH 6.0), 150 mM NaCl, with combinations of Co(II), Ni(II), and Zn(II), and measuring [metal] bound using atomic absorption spectrophotometry, following separation on Sephadex G-25.

Determination of Metal Quotas—Cells, R2-PIM8(*smt*) and *M. smegmatis* mc²155, were harvested during exponential growth and washed three times with 10 mM Tris-HCl (pH 7.5), 1 mM EDTA and once with Milli-Q H₂O. Pelleted cells were dried overnight at 80 °C, dissolved in 70% (v/v) nitric acid, and the metal content measured by atomic absorption spectrophotometry. Metal contents were determined as atoms mg⁻¹ cellular protein and atoms cell⁻¹ (from hemocytometer counts) or cyanobacterial cell volume equivalent for the mycobacteria as determined from packed cell volumes. Assays were performed in triplicate on at least three separate occasions, and parallel control experiments eliminated any metal contamination from the materials used.

Structural Model of NmtR—NmtR structure was modeled against SmtB (19) using SWISSMODEL (www.expasy.org/swissmod/ SWISS-MODEL.html).

RESULTS

NmtR Binds to the *nmt* Operator-Promoter Region and Is a Nickel- and Cobalt-responsive Repressor—Similarity of the deduced product of open reading frame Rv3744 (NmtR) to the zinc-responsive repressor SmtB (3), and of the divergently transcribed gene (*nmtA*) to metal-transporting P₁-type ATPases, suggests that the former might bind to the intervening operator-promoter region to regulate the latter. To test whether or not NmtR binds to the operator-promoter region

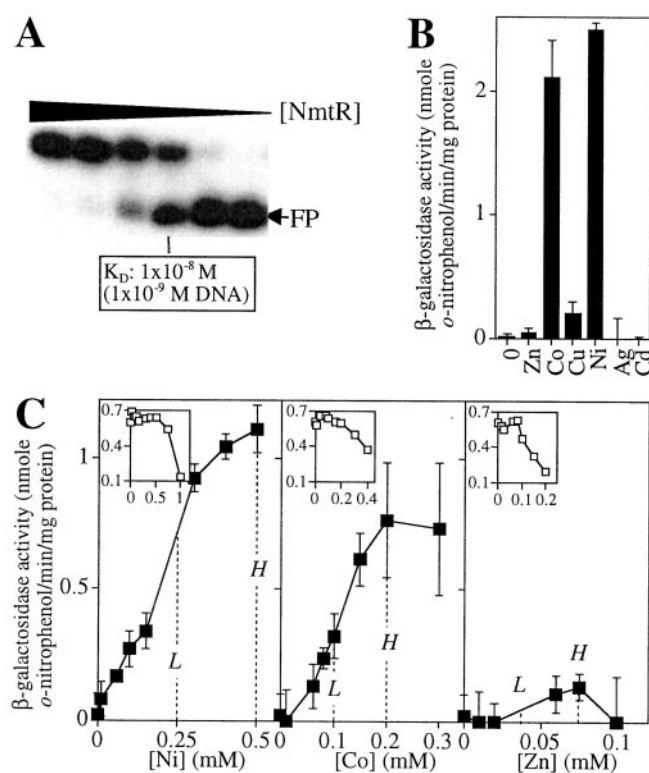


FIG. 2. NmtR binds to the *nmt* operator-promoter and responds to nickel and cobalt in a mycobacterium. *A*, gel retardation assays used 1×10^{-7} , 2.5×10^{-7} , 5×10^{-7} , 1×10^{-8} , 2×10^{-8} , or $4 \times 10^{-8} \text{ M}$ NmtR monomer (left to right) with $1 \times 10^{-9} \text{ M}$ *nmt* operator-promoter DNA as probe; the position of free probe (FP) is indicated. *B* and *C*, β -galactosidase activity in mycobacterial cells containing *nmtR*. Cells were grown with no metal supplement and maximum metal permissive [metal] (*B*) or up to inhibitory [Ni(II)], [Co(II)], or [Zn(II)] (*C*); maximum and half-maximum permissive [metal] are indicated (*H* and *L*, respectively). *Insets*, OD₅₉₅ cultures (y axis) against added [metal] (x axis).

separating *nmtR* and *nmtA* (Fig. 1C), NmtR was expressed in *E. coli*, purified, and used in gel retardation assays. A single retarded complex was detected (Fig. 2A), which was retained in the presence of nonspecific (poly(dI-dC)·poly(dI-dC)), but not specific (*nmt* operator promoter region), competitor DNA (data not shown).

NmtA shows greater similarity to the cobalt exporting P₁-type ATPase CoaT (27) than to related zinc exporters ZntA (34, 35) or ZiaA (4). It is probable that the same metals will be sensed by NmtR and transported by NmtA and therefore speculated that metal specificities of at least one of the proteins differ from those naively inferred from homologies. To establish which (if any) metals induce transcription from the *nmtA* operator-promoter, a 497-bp region including the operator-promoter region separating the two genes plus the entire *nmtR* coding region was fused to a promoterless *lacZ* in plasmid pJEM15 and introduced into *M. smegmatis* mc²155. Elevated β -galactosidase activity was detected in response to exposure (20 h) to maximum permissive concentrations of cobalt or nickel but no other metals (Fig. 2B). Elevated β -galactosidase activity in the absence of added metal ions was detected from an analogous construct in which codon Gln⁴¹ within the *nmtR* coding region had been converted to a stop codon, confirming that NmtR acts negatively toward expression from the *nmtA* operator-promoter. Exposure to a range of concentrations of zinc, cobalt, and nickel (Fig. 2C) revealed that no viable concentration (*insets* in Fig. 2C) of zinc induced expression from the *nmtA* operator-promoter, while nickel was the most potent inducer. Equivalent trends were observed in *M. bovis* BCG (not shown).

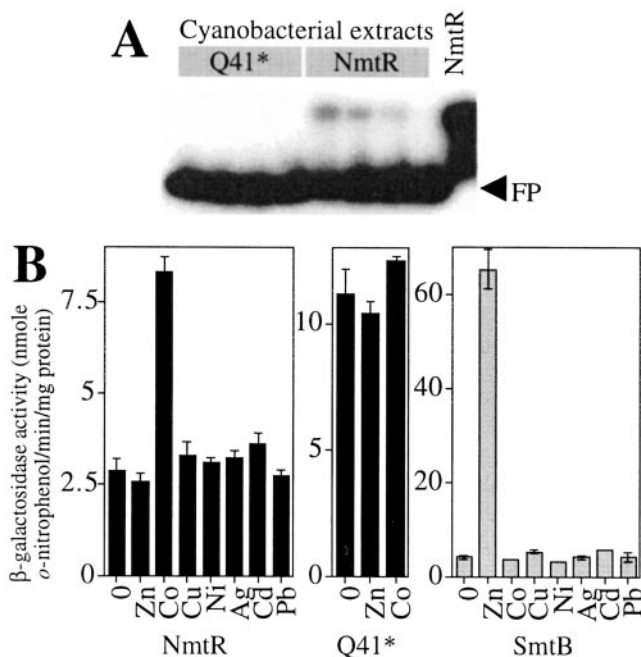


FIG. 3. *NmtR* and *SmtB* respond to different metal ions in a common host. *A*, gel retardation assays were performed using extracts ($\sim 40 \mu\text{g}$) from cyanobacteria containing *nmtR* (right box) or a stop-codon derivative (left box) or using recombinant *NmtR* ($1 \times 10^{-5} \text{ M}$) (far right) with $1 \times 10^{-9} \text{ M}$ *nmt* operator-promoter DNA as probe (FP, free probe). Each set of four reactions with cyanobacterial extracts contained (left to right) 0, 0.05, 0.1, or $0.2 \mu\text{g} \mu\text{l}^{-1}$ nonspecific competitor poly(dI-dC)·poly(dI-dC). *B*, β -galactosidase activity in the cyanobacterial cells used in *A*, containing *nmtR* (left) or the stop codon derivative (middle) or containing *smtB* (right). Cells were grown with no metal supplement and maximum permissible [metal].

In a Common Cell, R2-PIM8(smt), NmtR Responds to Cobalt and SmtB to Zinc—Differences in the metals that alleviate repression of transcription from the *nmtA* (Fig. 2) and *smtA* operator promoters (3) suggest that *NmtR* and *SmtB* can bind and/or allosterically respond to different metals. However, the promoters have been analyzed in different cell types, mycobacteria or cyanobacteria, where the abundance and/or chemical forms of the labile pools of these metal ions may differ. To investigate whether or not metal specificity is an intrinsic property of the sensors and/or influenced by the host cytosol, *nmt* reporter constructs were introduced into a cyanobacterium, R2-PIM8(*smt*), for direct comparison with *SmtB* in the same cell. Extracts from these cells formed complexes with the *nmt* operator-promoter in gel retardation assays; the complexes were absent when extracts were used from cells containing an equivalent construct with a stop codon in the *nmtR* open reading frame, confirming expression of *NmtR* in the heterologous host (Fig. 3A). In the absence of metal supplements, β -galactosidase activity was lower in cells with functional *nmtR* than *nmtR* containing a stop codon confirming *NmtR*-mediated repression (Fig. 3B). Exposure to maximum permissible concentrations of cobalt, but not zinc or any other tested metal, alleviated *NmtR*-mediated repression, while only zinc alleviated *SmtB*-mediated repression of expression from the *smtA* operator promoter under the same assay conditions (Fig. 3B). The two sensors show converse discrimination between cobalt and zinc in the same cytosol.

NmtR Does Not Respond to Nickel in R2-PIM8(smt) where the Nickel Content Is Lower and Less Variable than the Mycobacterium—Exposure to maximum permissible concentrations of nickel alleviated *NmtR*-mediated repression in the mycobacterium (Fig. 2B) but not in the cyanobacterium (Fig. 3B). To further investigate whether or not *NmtR* responds to nickel in

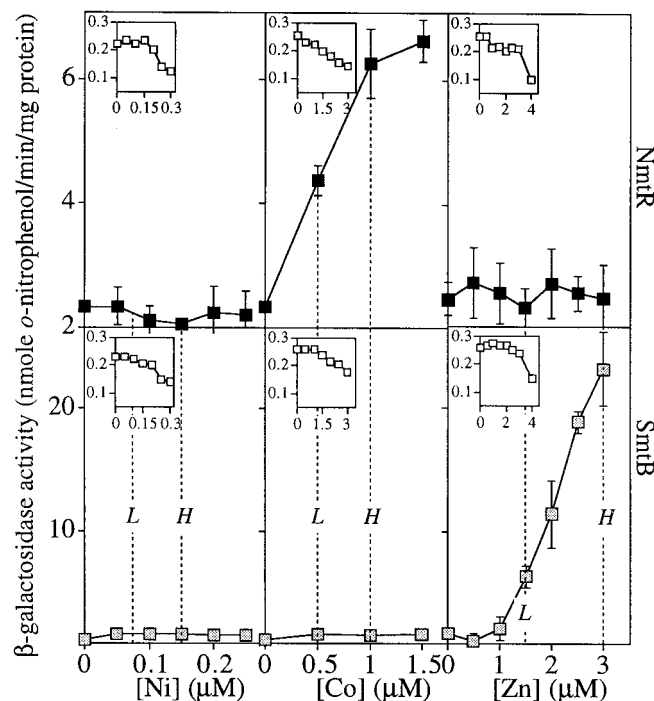


FIG. 4. Comparison of *NmtR* and *SmtB* metal specificities in a cyanobacterium. β -Galactosidase activity in cyanobacterial cells containing *nmtR* (upper) or *smtB* (lower) grown up to inhibitory [Ni(II)], [Co(II)], or [Zn(II)]; maximum and half-maximum permissible [metal] are indicated (H and L, respectively). Insets, OD_{595} cultures (y axis) against added [metal] (x axis).

the heterologous host, β -galactosidase activity was measured in response to a range of metal concentrations up to and including inhibitory doses (insets in Fig. 4). No increase was detected in response to any concentration of nickel, indicating a difference in the labile nickel pools of the two bacteria. *NmtR* only responded to cobalt, and *SmtB* to zinc, in the cyanobacterium (Fig. 4).

The nickel contents of both organisms were determined in cultures grown in normal medium or following supplementation with maximum permissible (labeled H on Figs. 2 and 4) or half-maximum permissible (L) nickel concentrations. Values were expressed as (i) number of atoms per cell (for the cyanobacterium) or per cyanobacterial cell volume equivalent for the mycobacterial cells and (ii) relative to protein content. These values increase by 37- and 38-fold in the mycobacterium but only 3.5- and 3-fold in the cyanobacterium following nickel supplementation. No increase was detected between half-maximum permissible and maximum permissible concentrations in the cyanobacterium. It is inferred that *NmtR* does not respond to nickel in the cyanobacterium, because the metal is excluded from the cell, relative to the mycobacterium.

SmtB Outcompetes NmtR for Zinc—Table I shows no significant increase in the zinc content of zinc-supplemented mycobacterial cells, but shows a greater than 10-fold increase in cyanobacteria. Exclusion of zinc from the mycobacterium could theoretically have accounted for the lack of a response of *NmtR* to zinc. Only by having established that *NmtR* also fails to respond to zinc in the cyanobacterium, where zinc is clearly available for detection by *SmtB* (Fig. 4), can it be concluded that this difference in selectivity reflects intrinsic differences between *SmtB* and *NmtR*. A simplistic explanation is that *SmtB* has a high affinity for zinc, low affinity for cobalt, and *NmtR* has a low affinity for zinc but high affinity for cobalt. The hierarchy of affinities for *SmtB* is $\text{Zn(II)} \gg \text{Co(II)} \gg \text{Ni(II)}$ (20). To establish the hierarchy of metal binding to *NmtR*, competitive binding experiments and direct titrations (see be-

TABLE I
Metal contents of mycobacterial and cyanobacterial cells

Cells were grown with no metal supplement (0), half-maximum (L), and maximum (H) permissive [Ni(II)], [Co(II)], or [Zn(II)]. Metal contents are shown as atoms mg^{-1} cellular protein or atoms cell^{-1} . Italicized values were close to the limits detectable under these experimental conditions.

[Metal]	Mycobacterial cells		Cyanobacterial cells	
	Atoms $\times 10^5$ cell^{-1a}	Atoms $\times 10^{15}$ mg protein^{-1}	Atoms $\times 10^5$ cell^{-1}	Atoms $\times 10^{15}$ mg protein^{-1}
Nickel				
0	0.2 (± 0.1)	0.1 (± 0.06)	0.2 (± 0.1)	0.1 (± 0.04)
L	3.6 (± 0.3)	1.8 (± 0.1)	0.7 (± 0.1)	0.3 (± 0.03)
H	7.4 (± 0.6)	3.8 (± 0.3)	0.7 (± 0.5)	0.3 (± 0.2)
Cobalt				
0	0.2 (± 0.02)	0.1 (± 0.01)	0.3 (± 0.1)	0.1 (± 0.04)
L	0.7 (± 0.1)	0.4 (± 0.1)	5.3 (± 0.6)	2.0 (± 0.2)
H	1.2 (± 0.1)	0.6 (± 0.1)	11.5 (± 0.1)	4.3 (± 0.04)
Zinc				
0	3.4 (± 0.9)	1.7 (± 0.5)	0.8 (± 0.2)	0.4 (± 0.1)
L	2.8 (± 0.6)	1.4 (± 0.3)	6.5 (± 1.1)	2.4 (± 0.4)
H	3.7 (± 0.5)	1.8 (± 0.3)	8.5 (± 0.3)	3.1 (± 0.1)

^a Metal contents are shown as cyanobacterial cell volume equivalents for the mycobacteria.

low) were performed. Apo-NmtR was incubated with an excess (with respect to protein) of equimolar amounts of each paired combination of these ions, fractionated on Sephadex G-25, bound and free metal quantified by atomic absorption spectrophotometry to determine which ion was predominantly bound and indicating the order $\text{Zn(II)} > \text{Ni(II)} \gg \text{Co(II)}$. It is possible that while both proteins bind zinc with highest affinity only SmtB can compete with endogenous ligands, implying that NmtR binds zinc with lower affinity than SmtB. The two $\alpha 5$ sites of SmtB, which mediate zinc-dependent DNA dissociation, have $K_{\text{Zn}} \approx 7.8 \times 10^{11} \text{ M}^{-1}$. The $\alpha 3\text{N}$ sites that are occupied in free solution have K_{Zn} of at least 10^{13} M^{-1} (21). The zinc-binding site(s) of NmtR remain to be defined, and K_{Zn} may also exceed 10^{13} M^{-1} ; competitive binding was therefore used to directly establish which protein preferentially acquires zinc.

Cobalt-SmtB is blue with distinctive spectral features around 550 nm, and between 300 and 400 nm (20). In contrast, cobalt-NmtR is nearly colorless with molar absorptivities in the visible region of $\leq 100 \text{ M}^{-1} \text{ cm}^{-1}$ (see below). Addition of zinc displaces cobalt and thereby bleaches cobalt-SmtB (20). Zinc-mediated bleaching of cobalt-SmtB was unaffected by the presence of an equimolar amount of NmtR (Fig. 5), establishing that zinc binds to SmtB in preference to NmtR and implying a difference in affinity of at least one order of magnitude.

At Equivalent Concentrations Cobalt, but Not Zinc, Cause Dissociation of NmtR from DNA—Of the three ions tested, zinc binds to NmtR with the highest affinity, cobalt the lowest, and yet the latter alleviates NmtR-mediated repression *in vivo* but the former does not (Fig. 4). Perhaps cobalt-NmtR undergoes an allosteric change to impair DNA binding, while zinc-NmtR does not. This was tested in gel retardation assays. Purified NmtR remains associated with *nmt* operator-promoter DNA in the presence of zinc at concentrations where cobalt inhibits complexes (Fig. 6). Higher zinc concentrations inhibited the formation of NmtR DNA complexes, but this requires further investigation due to evidence of protein precipitation. Preliminary titration of DNA with preformed complexes of apo-, cobalt-, nickel-, or zinc-NmtR, monitored via fluorescence anisotropy, was also consistent with nickel and cobalt similarly regulating complex formation with both metals more effective than zinc (data not shown).

Identification of Six $\alpha 5\text{C}$ Residues That Are Essential for Nickel and Cobalt Sensing by NmtR—Some difference in the effector recognition site of NmtR compared with SmtB might (i) favor binding of nickel over cobalt, (ii) disfavor binding of zinc

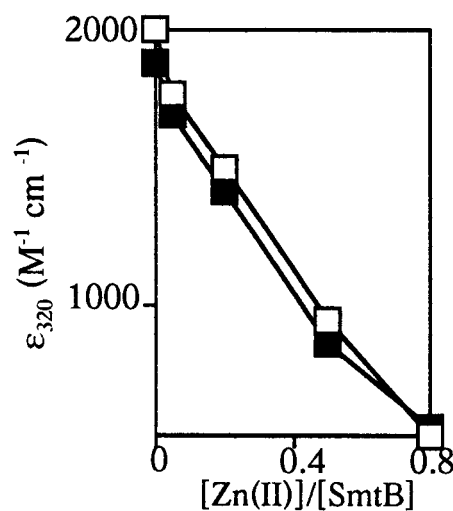


FIG. 5. Zinc binds to SmtB in preference to NmtR. Zn(II) displacement binding isotherm for Co(II)-substituted SmtB, plotted as ϵ_{320} against total $[\text{Zn(II)}]/[\text{SmtB monomer}]$ with (closed symbols) or without (open symbols) stoichiometric amounts of NmtR present.

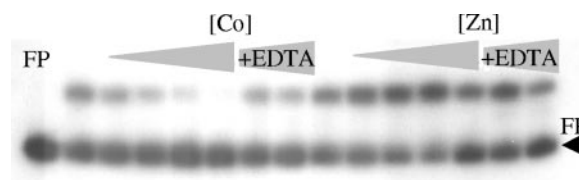


FIG. 6. Cobalt inhibits NmtR binding to *nmt* operator-promoter DNA more effectively than zinc *in vitro*. Gel retardation assays were performed using $1 \times 10^{-9} \text{ M}$ *nmt* operator-promoter DNA as probe (FP, free probe) and $1 \times 10^{-8} \text{ M}$ NmtR with (left to right) 0, 1×10^{-5} , 2.5×10^{-5} , 5×10^{-5} , or $7.5 \times 10^{-5} \text{ M}$ Co(II) or Zn(II) added to binding reactions. EDTA (1 mM) was subsequently added to duplicate reactions containing 5×10^{-5} or $7.5 \times 10^{-5} \text{ M}$ Co(II) or Zn(II) as indicated.

in competition with SmtB (Fig. 5B), and/or (iii) favor allosteric regulation by nickel and cobalt in preference to zinc (Fig. 6). The next challenge was to identify the inducer recognition site of NmtR. Asp⁵¹ in NmtR aligns with conserved Asp residues in other family members (8) and, at least in SmtB, is thought to contribute one $\alpha 3\text{N}$ ligand (21). Ala substitution of Asp⁵¹ did not impair either NmtR-mediated repression or nickel/cobalt recognition (Fig. 7). Inducer recognition by NmtR either does not involve $\alpha 3\text{N}$ sites, or Asp⁵¹ is not an essential $\alpha 3\text{N}$ ligand.

While inducer recognition by many ArsR-SmtB family members requires $\alpha 3\text{N}$ sites (8, 23), in SmtB ligands from antiparallel $\alpha 5$ helices at the carboxyl-terminal dimer interface are obligatory for metal-mediated DNA dissociation (21). The $\alpha 5$ helices of NmtR were predicted based upon the coordinates for SmtB, and Fig. 7 shows a hypothetical dimer interface at the carboxyl-terminal region of NmtR. Four candidate nickel/cobalt ligands in NmtR, Asp⁹¹, His⁹³, His¹⁰⁴, and His¹⁰⁷ (Fig. 7) correspond to the $\alpha 5$ residues Asp¹⁰⁴, His¹⁰⁶, His¹¹⁷, and Glu¹²⁰ of SmtB (Fig. 1A). Substitution of any one of these residues in NmtR created functional repressors that mediated low expression of *lacZ* from the *nmtA* operator-promoter in mycobacterial cells grown in the absence of metal supplements. In contrast β -galactosidase activity was constitutively elevated in cells containing a non-functional mutant in which the codon for Gln⁴¹ had been substituted with a stop codon. Most importantly, substitution of NmtR residues aligning with the $\alpha 5$ ligands of SmtB caused loss of inducer recognition with β -galactosidase activity remaining low in the presence of nickel and cobalt concentrations that cause loss of repression by wild-type NmtR.

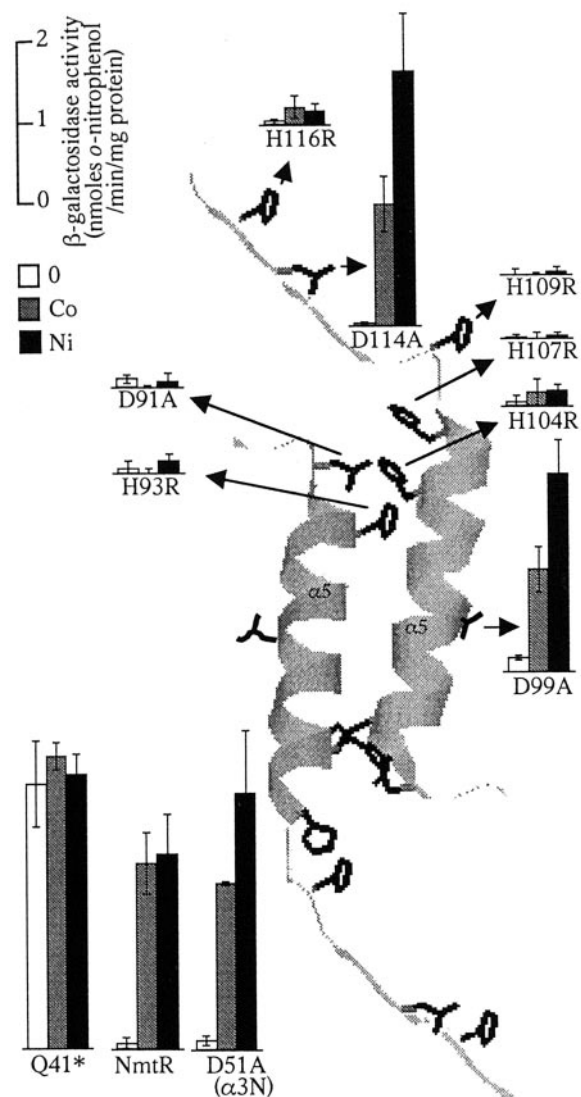


FIG. 7. **Metal-sensing residues of NmtR.** A, ribbon representation of the $\alpha 5$ helices and eleven additional (to SmtB) residues at NmtR carboxyl terminus with side chains of Asp⁹¹, His⁹³, Asp⁹⁹, His¹⁰⁴, His¹⁰⁷, His¹⁰⁹, Asp¹¹⁴, and His¹¹⁶ is shown. β -Galactosidase activity was measured in mycobacterial cells containing wild-type *nmtR* and various derivatives, coding for indicated mutant proteins, grown with no metal supplement or maximum permissible [Co(II)] or [Ni(II)].

NmtR has 11 additional carboxyl-terminal residues relative to SmtB (drawn as unstructured ribbon on Fig. 7), including three additional potential nickel/cobalt ligands, His¹⁰⁹, Asp¹¹⁴, and His¹¹⁶. Substitution of Asp¹¹⁴ had no detectable effect on repression or inducer recognition, but substitution of either His created inducer non-responsive functional repressors, thereby identifying a total of six residues, all of which are obligatory for either cobalt or nickel recognition (Fig. 7).

UV-visible Absorption Spectroscopy of Ni(II)- and Co(II)-substituted NmtR—Site-directed mutagenesis of NmtR (Fig. 7) suggests that inducer recognition could involve hexadentate Ni(II) or Co(II) coordination complexes formed by extended carboxyl-terminal $\alpha 5C$ sites in a way in which six ligands (rather than four for SmtB) are required for allosteric regulation of DNA binding, and thus sensing. Consistent with this, the saturated UV-visible absorption spectrum of Ni(II)-NmtR (Fig. 8A) recorded at a 1:1 Ni(II)-NmtR monomer ratio reveals three very weak ($\epsilon \leq 80 \text{ M}^{-1} \text{ cm}^{-1}$) and very broad ligand field absorption transitions diagnostic (36) of six-coordinate d^8 Ni(II). It is noted that the gradual upward slope in the cor-

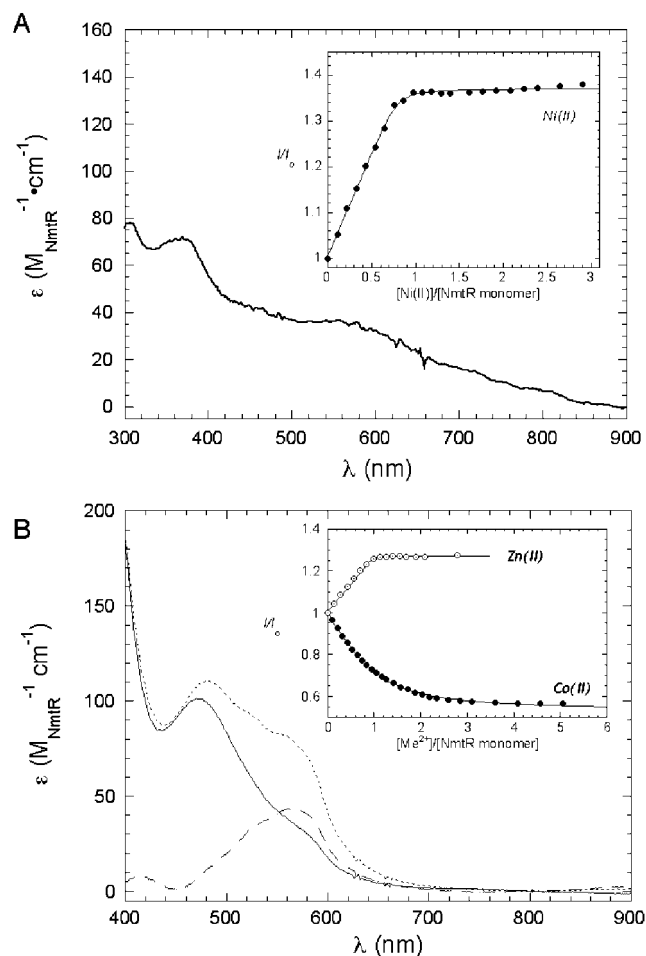


FIG. 8. **Spectroscopic analysis of metallated NmtR.** A, electronic molar absorptivity spectrum of Ni(II)-NmtR (1:1 molar ratio of Ni(II):NmtR monomer or two per dimer). *Inset*, Ni(II) binding isotherm as monitored by tyrosine fluorescence ($\lambda_{\text{ex}} = 280 \text{ nm}$; $\lambda_{\text{em}} = 305 \text{ nm}$) with the solid line representing a fit to a 1:1 (metal:monomer) binding model ($n = 0.8$, $K_{\text{Ni}} = 2.6 (\pm 0.7) \times 10^7 \text{ M}^{-1}$). B, electronic molar absorptivity spectrum of Co(II)-NmtR obtained with molar ratios of 0.5:1 (1 metal per dimer; solid line) and 1:1 (2 metals per dimer; dotted line) Co(II):NmtR monomer, as well as a difference spectrum characteristic of the binding of the second Co(II) to the dimer (dashed line). Further additions of Co(II) caused no additional changes in the spectra (data not shown). *Inset*, Co(II) and Zn(II) binding isotherms as monitored by tyrosine fluorescence with the solid lines representing fits to a 1:1 binding model for Co(II) ($K_{\text{Co}} = 7.1 (\pm 0.3) \times 10^5 \text{ M}^{-1}$) and Zn(II) ($K_{\text{Zn}} = 1.5 (\pm 2.3) \times 10^8 \text{ M}^{-1}$). K_{Ni} and K_{Zn} are too tight to measure under these conditions and represent only lower limits. Conditions: 10 mM HEPES, 0.45 M NaCl (pH 7.0), 22 °C.

rected spectrum of Ni(II)-NmtR is not due to light scattering, but rather to the non-resolved nature of low intensity absorption bands characteristic of Ni(II) in coordination complexes deviating from perfect trigonal bipyramidal or octahedral coordinate symmetry (37). The *inset* (Fig. 8A) reveals that the stoichiometry of Ni(II) binding to NmtR is 1 Ni(II) per monomer or 2 per dimer (NmtR is fully dimeric under these conditions)² with a lower limit of the affinity for Ni(II), $K_{\text{Ni}} \geq 2 \times 10^7 \text{ M}^{-1}$. For SmtB, $K_{\text{Ni}} = 1.7 (\pm 0.4) \times 10^5 \text{ M}^{-1}$ (20). Analogous data are shown for Co(II)-substituted NmtR in Fig. 8B. Although both 1:1 and 2:1 Co(II):NmtR dimer complexes are spectroscopically distinct (in contrast to Ni(II) complexes), the low molar absorptivities of each complex are indicative of five- or six-coordinate d^7 Co(II) (38); the spectrum that characterizes the second bound Co(II) is nearly superimposable with other octa-

² M. A. Pennella and D. P. Giedroc, unpublished observations.

hedral Co(II) complexes described in the literature (39). Consistent with the competitive metal binding experiments described above, Co(II) binds to NmtR with an affinity ≥ 40 -fold weaker than Ni(II) and at least 500-fold weaker than Zn(II) (*inset*, Fig. 8B) again implying that for NmtR, $K_{Zn} \geq K_{Ni} > K_{Co}$. Remarkably, K_{Co} for NmtR is ≈ 3000 -fold smaller for NmtR relative to SmtB under similar solution conditions (20, 21) despite the finding that NmtR senses Co(II), while SmtB does not (Fig. 3).

DISCUSSION

Several lines of evidence demonstrate that NmtR is a nickel/cobalt-responsive DNA-binding repressor of transcription from the divergent *nmtA* operator-promoter. (i) Purified NmtR forms specific complexes with the *nmtA* operator promoter *in vitro* (Fig. 2A); (ii) equivalent complexes are detected using crude lysates of R2-PIM8(*smt*) containing *nmtR* but not cells containing an internal stop codon in *nmtR* (Fig. 3A); (iii) expression of β -galactosidase activity from the *nmtA* operator-promoter is elevated in mycobacterial (Fig. 7) and cyanobacterial (Fig. 3) cells devoid of functional *nmtR* compared with cells containing NmtR; (iv) expression of β -galactosidase activity via the *nmtA* operator-promoter is elevated in both bacterial cell types in response to elevated cobalt (Figs. 2 and 3), and nickel is the most potent inducer at viable concentrations in the mycobacterium (Fig. 2). Factors that contribute to metal selectivity in the context of a cell have been identified, *i.e.* which metals are detected by NmtR or SmtB.

The most potent allosteric effector of NmtR (nickel) in mycobacteria (Fig. 2C) is totally ineffective when *nmtR* is introduced into a cyanobacterium (Fig. 4). Clearly NmtR is produced and accumulated in the cyanobacterium (Fig. 3A), is functional as a repressor (Fig. 3B), and is competent to detect metal (cobalt) but unable to acquire and detect nickel even at concentrations inhibitory to cell growth (Fig. 4). These observations demonstrate that different cytosolic metal pools can determine the metals that metallo-sensory proteins detect in different cells. By analogy, cadmium and copper are the most potent inducers of dMTF-1 in *Drosophila*, but in transfected mammalian cells dMTF-1 responds to zinc, similar to its mammalian counterpart (40). In theory, related sensors from different bacteria responding to alternative metals *in vivo* could have identical metal-binding sites, identical allosteric responses to metals *in vitro*, but "restricted access" to different available metal pools *in vivo*.

Loss of nickel induction in R2-PIM8(*smt*) could indicate that a nickel metallochaperone for NmtR is absent in the cyanobacterium, suggesting a technical basis for selective screens for metallochaperones. However, cell nickel quotas (Table I) establish that more effective exclusion of nickel from the cyanobacterial, compared with mycobacterial, cytosol can account for the cellular differences observed here. Strikingly, SmtB does not respond to cobalt in the cyanobacterium even though it is intrinsically capable of allosterically responding to cobalt *in vitro* (22), and cobalt is available for detection in the cell at least by NmtR (Fig. 4); furthermore, SmtB binds Co(II) with a far greater affinity than does NmtR (Fig. 8). Although the nature of the available cobalt pool is unknown (association with proteins of cobalamin biosynthesis seems likely), these data imply that NmtR acquires cobalt from this pool far more effectively than does SmtB.

Crucially, SmtB and NmtR detect different metals (zinc and cobalt) when analyzed in the same cell type (Fig. 4) establishing that intrinsic features of these two proteins discriminate in favor of different metals. Most importantly this is not solely based on absolute binding preferences, since SmtB and NmtR both have higher affinities for zinc than for cobalt or nickel

(Fig. 6), and two contributory factors have been identified. (i) SmtB outcompetes NmtR for zinc (Fig. 5) and could therefore more readily acquire zinc from other ligands in the cytosol. (ii) Zinc mediates allosteric regulation of DNA binding ineffectively (Fig. 6).

Why is cobalt (and nickel) more effective than zinc at promoting DNA dissociation by NmtR? NmtR absorption spectra are indicative of distorted octahedral Ni(II) coordination and five- or six-coordinate Co(II) liganding (Fig. 8). In contrast, SmtB is characterized by four-coordinate, tetrahedral complexes of both Co(II) and Zn(II) (20, 21). Although the coordination geometry of Zn(II)-NmtR is not yet known, at least one explanation is that the difference in the allosteric regulation of DNA binding by NmtR *versus* SmtB requires metal coordination bonds to six protein-derived ligands, rather than four. This is consistent with the identification of six potential ligands by site-directed mutagenesis, each obligatory for inducer recognition *in vivo*. Ni(II) and Co(II) show a greater propensity to form octahedral coordination complexes relative to Zn(II) (11), and this is the most common geometry for Ni(II) and Co(II) catalogued in protein structural databases (12); in contrast, tetrahedral coordination geometry predominates for Zn(II) (12). Consistent with these trends, Zn(II) complexes of *E. coli* glyoxalase are five-coordinate and catalytically inactive, whereas the Ni(II) and Co(II) complexes recruit an additional water molecule into the first coordination sphere creating a nearly perfect octahedral complex, which exhibits high catalytic activity (41). It is tempting to speculate that two additional ligands provided by the COOH-terminal extension of the $\alpha 5$ helices in NmtR (Fig. 7) adapt negative regulation of operator/promoter binding previously observed for SmtB (22) to require hexadentate metal ligation environments. Metal detection within a cell might therefore be achieved in the absence of strict discrimination at the level of protein-metal binding. It remains unknown why the higher affinity zinc does not associate with NmtR *in vivo* in such a way that detection of nickel and cobalt is inhibited. This work highlights the need to identify the chemical form(s) of the labile pool(s) of metals accessible by each metal sensor and indeed other metalloproteins.

Acknowledgments—We thank Pamela Robinson for proof reading the manuscript, Chris Dennison for early insights regarding coordination geometries, Del Besra for advice on the genetic manipulation of mycobacteria, and R. J. P. Williams for comments on a draft manuscript.

REFERENCES

- O'Halloran, T. V. (1993) *Science* **261**, 715–725
- Robinson, N. J., Whitehall, S. K., and Cavet, J. S. (2001) *Adv. Microbial Physiol.* **44**, 183–213
- Huckle, J. W., Morby, A. P., Turner, J. S., and Robinson, N. J. (1993) *Mol. Microbiol.* **7**, 177–187
- Thelwell, C., Robinson, N. J., and Turner-Cavet, J. S. (1998) *Proc. Natl. Acad. Sci. U. S. A.* **95**, 10728–10733
- Xu, C., Shi, W., and Rosen, B. P. (1996) *J. Biol. Chem.* **271**, 2427–2432
- Endo, G., and Silver, S. (1995) *J. Bacteriol.* **177**, 4437–4441
- Sun, Y., Wong, M. D., and Rosen, B. P. (2001) *J. Biol. Chem.* **276**, 14955–14960
- Busenlehner, L. S., Weng, T.-C., Penner-Hahn, J. E., and Giedroc, D. P. (2002) *J. Mol. Biol.* **319**, 685–701
- Singh, V. K., Xiong, A., Usgaard, T. R., Chakrabarti, S., Deora, R., Misra, T. K., and Jayaswal, R. K. (1999) *Mol. Microbiol.* **33**, 200–207
- Kuroda, M., Hayashi, H., and Ohta, T. (1999) *Microbiol. Immunol.* **43**, 115–125
- Frausto da Silva, J. J. R., and Williams, R. J. P. (2001) *The Biological Chemistry of the Elements: The Inorganic Chemistry of Life*, 2nd Ed, Clarendon Press, Oxford, UK
- Rulisek, L., and Vondrásek, J. (1998) *J. Inorg. Biochem.* **71**, 115–127
- Rae, T. D., Schmidt, P. J., Pufahl, R. A., Culotta, V. C., and O'Halloran, T. V. (1999) *Science* **284**, 805–808
- Outten, C. E., and O'Halloran, T. V. (2001) *Science* **292**, 2488–2492
- Hausinger, R. P. (1997) *J. Biol. Inorg. Chem.* **2**, 279–286
- O'Halloran, T. V., and Culotta, V. C. (2000) *J. Biol. Chem.* **275**, 25057–25060
- Totter, S., Rondet, S. A. M., Borrelly, G. P. M., Robinson, P. J., Rich, P. R., and Robinson, N. J. (2002) *J. Biol. Chem.* **277**, 5490–5497
- Turner, J. S., Glands, P. D., Samson, A. C. R., and Robinson, N. J. (1996) *Nucleic Acids Res.* **24**, 3714–3721
- Cook, W. J., Kar, S. R., Taylor, K. B., and Hall, L. M. (1998) *J. Mol. Biol.* **275**, 337–347
- VanZile, M. L., Cosper, N. J., Scott, R. A., and Giedroc, D. P. (2000) *Biochem-*

- istry **39**, 11818–11829
21. VanZile, M. L., Chen, X., and Giedroc, D. P. (2002) *Biochemistry* **41**, 9765–9775
22. VanZile, M. L., Chen, X., and Giedroc, D. P. (2002) *Biochemistry* **41**, 9776–9786
23. Shi, W., Dong, J., Scott, R. A., Ksenzenko, M. Y., and Rosen, B. P. (1996) *J. Biol. Chem.* **271**, 9291–9297
24. Busenlehner, L. S., Cospier, N. J., Scott, R. A., Rosen, B. P., Wong, M. D., and Giedroc, D. P. (2001) *Biochemistry* **40**, 4426–4436
25. Outten, C. E., Tobin, D. A., Penner-Hahn, J. E., and O'Halloran, T. V. (2001) *Biochemistry* **40**, 10417–10423
26. Cole, S. T., Brosch, R., Parkhill, J., Garnier, T., Churcher, C., Harris, D., Gordon, S. V., Eiglmeier, K., Gas, S., Barry, C. E., 3rd, Tekaiia, F., Badcock, K., Basham, D., Brown, D., Chillingworth, T., *et al.* (1998) *Nature* **393**, 537–544
27. Rutherford, J. C., Cavet, J. S., and Robinson, N. J. (1999) *J. Biol. Chem.* **274**, 25827–25832
28. Gordon, S. V., Brosch, R., Billault, A., Garnier, T., Eiglmeier, K., and Cole, S. T. (1999) *Mol. Microbiol.* **32**, 643–655
29. Turner, J. S., Morby, A. P., Whitton, B. A., Gupta, A., and Robinson, N. J. (1993) *J. Biol. Chem.* **268**, 4494–4498
30. Sambrook, J., Fritsch, E. F., and Maniatis, T. (1989) *Molecular Cloning: A Laboratory Manual*, 2nd Ed, Cold Spring Harbor Laboratory, Cold Spring Harbor, NY
31. Timm, J., Lim, E. M., and Gicquel, B. (1994) *J. Bacteriol.* **176**, 6749–6753
32. Scanlan, D. J., Bloye, S. A., Mann, N. H., Hodgson, D. A., and Carr, N. G. (1990) *Gene (Amst.)* **90**, 43–49
33. Morby, A. P., Turner, J. S., Huckle, J. W., and Robinson, N. J. (1993) *Nucleic Acids Res.* **21**, 921–925
34. Beard, S. J., Hashim, R., Membrillo-Hernandez, J., Hughes, M. N., and Poole, R. K. (1997) *Mol. Microbiol.* **25**, 883–891
35. Rensing, C., Mitra, B., and Rosen, B. P. (1997) *Proc. Natl. Acad. Sci. U. S. A.* **94**, 14326–14331
36. Rosa, D. T., Krause Bauer, J. A., and Baldwin, M. J. (2001) *Inorg. Chem.* **40**, 1606–1613
37. Posewitz, M. C., and Wilcox, D. E. (1995) *Chem. Res. Toxicol.* **8**, 1020–1028
38. Corwin, D. T., Jr., Fikar, R., and Koch, S. A. (1987) *Inorg. Chem.* **26**, 3079–3080
39. Bicknell, R., Henson, G. R., Holmquist, B., and Little, C. (1986) *Biochemistry* **25**, 4219–4223
40. Zhang, B., Egli, D., Georiev, O., and Schaffner, W. (2001) *Mol. Cell. Biol.* **21**, 4505–4514
41. He, M. M., Clugston, S. L., Honek, J. F., and Matthews, B. W. (2000) *Biochemistry* **39**, 8719–8727